

PS Plan-View Paleochannel Reconstruction of Ancient Meanderbelts, Cretaceous Ferron Sandstone, Henry Mountains Region, Utah*

Jianqiao Wang¹ and Janok P. Bhattacharya²

Search and Discovery Article #51122 (2015)**

Posted August 17, 2015

*Adapted from poster presentation given at AAPG 2015 Annual Convention and Exhibition, Denver, Colorado, May 31 – June 3, 2015

**Datapages © 2015 Serial rights given by author. For all other rights contact author directly.

¹Colorado School of Mines, Golden, Colorado, USA (jiawang@mines.edu)

²School of Geography & Earth Sciences, McMaster University, Hamilton, Ontario, Canada

Abstract

Few studies on reconstructing paleohydraulic parameters of ancient rivers obtained from outcrops have been examined by plan-view characteristics (meander amplitude and sinuosity). Plan view and cliff exposures of amalgamated ancient meander belts in the Cretaceous Ferron Sandstone member, Mancos Shale Formation, Utah, allow paleohydraulic reconstruction based on both vertical and plan-view outcrop data, evaluation of numerical models of facies variability in meander belts, as well as addressing the variability of paleocurrents and facies heterogeneity in complex fluvial analog reservoirs. This project integrates 3 measured sections from cliff facies, plan-view interpretive maps made from aerial photos, with 1259 areal grain-size measurements, 800 paleocurrents (mostly rib and furrows from dunes) and 75 strike and dip measurements on exposed bar accretion surfaces. Three amalgamated channel belts are marked by scour surfaces, an increase in grain size, and abrupt changes in paleocurrent orientations. The youngest is 2.0 m in depth, 90m in width, 435m in meander amplitude, and has a sinuosity of 2.9. The middle is 3.1m in depth, 1083m in meander amplitude, and has a sinuosity of 1.2. The oldest was insufficiently exposed to document its plan view style. Grain size showed systematic fining-upwards within each channel story, coarsening towards the bend apex along the bend axis, and fining downstream within some meander scrolls. Plan-form trends were less well developed, perhaps reflecting the fact that the exposures capture variable vertical position within the belts. Paleocurrents showed systematically varying trends within belts (from NE, to SW, to E), with abrupt changes between belts. Grain size and vertical facies associations vary as a function of the style of bar migration, as well as position within a bar (upstream vs. downstream). The outcrop showed the dominance of a meandering river style overall, according to lateral amalgamation of successive point bars within the belts. Compound braid bars, built by overlapping unit bars, constitute the youngest channel deposits, probably associated with channel abandonment. Independent measurements of meander wavelength based on plan view exposures match results from empirical equations. The Ferron rivers are small to medium in scale according to calculated paleohydraulic parameters ($Q_w = 135\sim 225\text{m}^3/\text{sec}$).



Plan-View Paleochannel Reconstruction of Ancient Meanderbelts, Cretaceous Ferron Sandstone, Henry Mountains Region, Utah

Jianqiao Wang¹, Janok Bhattacharya²

1. Colorado School of Mines, Golden, CO, United States. 2. School of Geography & Earth Sciences, McMaster University, Hamilton, ON, Canada

ABSTRACT

Few studies on reconstructing paleohydraulic parameters of ancient rivers obtained from outcrops have been examined by plan-view characteristics (meander amplitude and sinuosity). Plan view and cliff exposures of amalgamated ancient meander belts in the Cretaceous Ferron Sandstone member, Mancos Shale Formation, Utah, allow paleohydraulic reconstruction based on both vertical and plan-view outcrop data, evaluation of numerical models of facies variability in meander belts, as well as addressing the variability of paleocurrents and facies heterogeneity in complex fluvial analog reservoirs.

This project integrates 3 measured sections from cliff facies, plan-view interpretive maps made from aerial photos, with 1259 areal grain-size measurements, 800 paleocurrents (mostly rib and furrows from dunes) and 75 strike and dip measurements on exposed bar accretion surfaces. Three amalgamated channel belts are marked by scour surfaces, an increase in grain size, and abrupt changes in paleocurrent orientations. The youngest is 2.0 m in depth, 90m in width, 435m in meander amplitude, and has a sinuosity of 2.9. The middle is 3.1m in depth, 1083m in meander amplitude, and has a sinuosity of 1.2. The oldest was insufficiently exposed to document its plan view style. Grain size showed systematic fining-upwards within each channel story, coarsening towards the bend apex along the bend axis, and fining downstream within some meander scrolls. Plan-form trends were less well developed, perhaps reflecting the fact that the exposures capture variable vertical position within the belts. Paleocurrents showed systematically varying trends within belts (from NE, to SW, to E), with abrupt changes between belts.

Grain size and vertical facies associations vary as a function of the style of bar migration, as well as position within a bar (upstream vs. downstream). The outcrop showed the dominance of a meandering river style overall, according to lateral amalgamation of successive point bars within the belts. Compound braid bars, built by overlapping unit bars, constitute the youngest channel deposits, probably associated with channel abandonment. Independent measurements of meander wavelength based on plan view exposures match results from empirical equations. The Ferron rivers are small to medium in scale according to calculated paleohydraulic parameters ($Qw = 135\text{--}225\text{m}^3/\text{sec}$).

METHODOLOGY

Tasks include taking measurement along transects marked in plan view and associated cliff view. Locations of measured sites were tracked by GPS. A Jacob's staff is used together with geological hammer, hand lens, and grain-size chart to obtain key data. Physical features of the rock, such as grain size and sedimentary structures were noted along each transect (about 15m apart along a given transect).

- Grid lines were set up by using Google Earth map and ArcMap in a World Geodetic System 1984, and the systematic grid was walked out during data measurement. Density of data is constrained by the time spending in field. Space is about 25~50m wide between every two adjacent transects. Result of this study shows the spacing is close enough to investigate and observe boundaries separating bar assemblages.
- A total of 1259 grain-size samples were taken from bar surfaces about every 15m along each transect in channel belt A1 and A2. Grain size and elevations of bar deposits are all marked in tens to hundreds of meter increments. Some can be clearly delineated by examining the geometry in outcrop.
- A total of 800 paleocurrent measurements in plan view were taken. Paleocurrent direction measurements were obtained wherever rib and furrows structures are well exposed.
- Strike and dip measurements of about 75 accretion beds were also taken.

Plan-view reconstruction of bars and channels was made by integrating the above data. The geometry of successive accretion surfaces within a bar deposit was obtained in plan-view and cross sectional exposures to determine whether it represents lateral, downstream, or upstream accretion. Accretion beds and widths of cross beds ribs were noted to define ancient unit bars and in order to examine the accretion topography within meander scrolls. Bedding architecture and paleocurrents can be used to distinguish longitudinal and/or transverse bars in braided rivers, versus migrating point bars in meandering rivers.

Additionally, the plan-view and cross-sectional outcrops provide more 3-dimensional data to estimate the original bankfull depth of the Ferron rivers. Paleohydraulic parameters were directly estimated, allowing comparison of sandstone width, thickness, and meander wavelength to empirical equations.

STUDY AREA

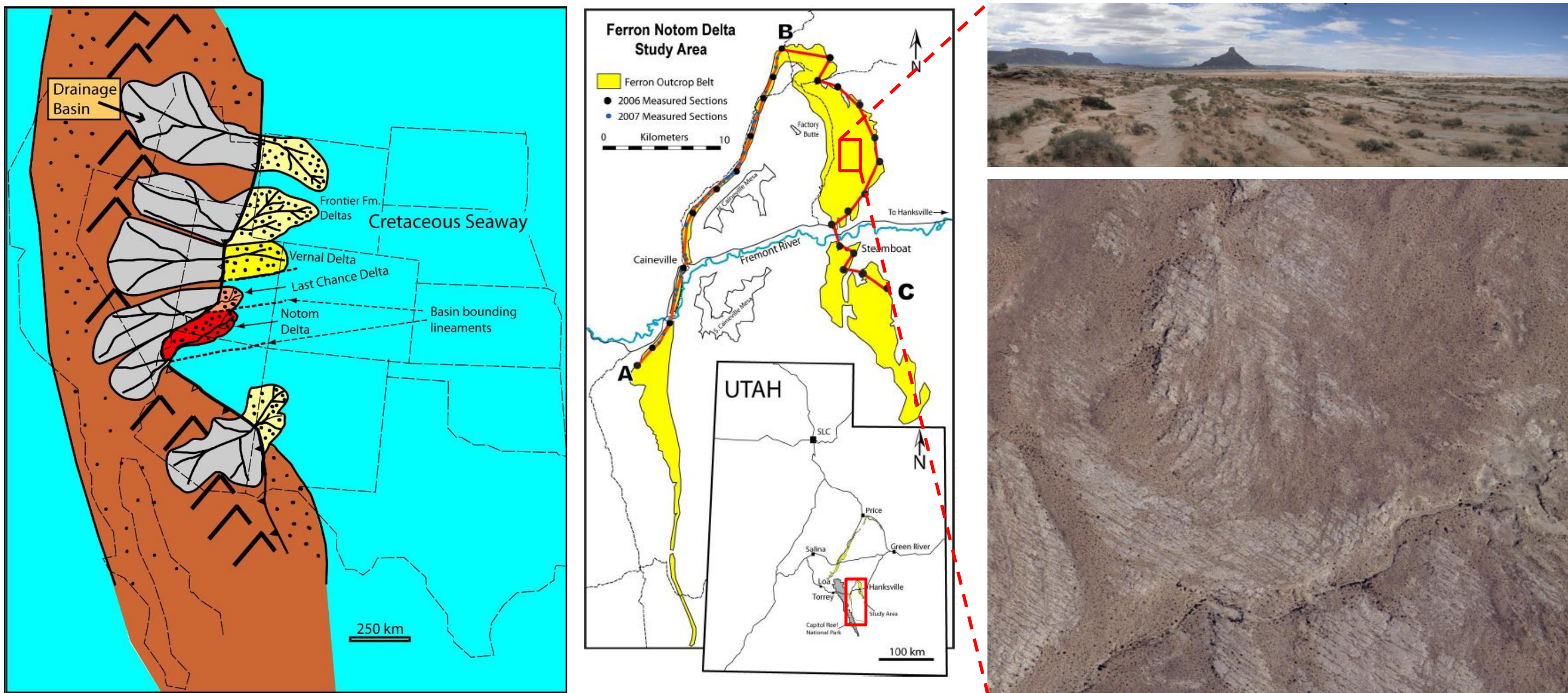


Figure. Paleogeographic reconstruction map of mid-Cretaceous Ferron Delta Complexes. Bhattacharya and Tye (2004) based on Gardner (1995) and Stelck (1975)

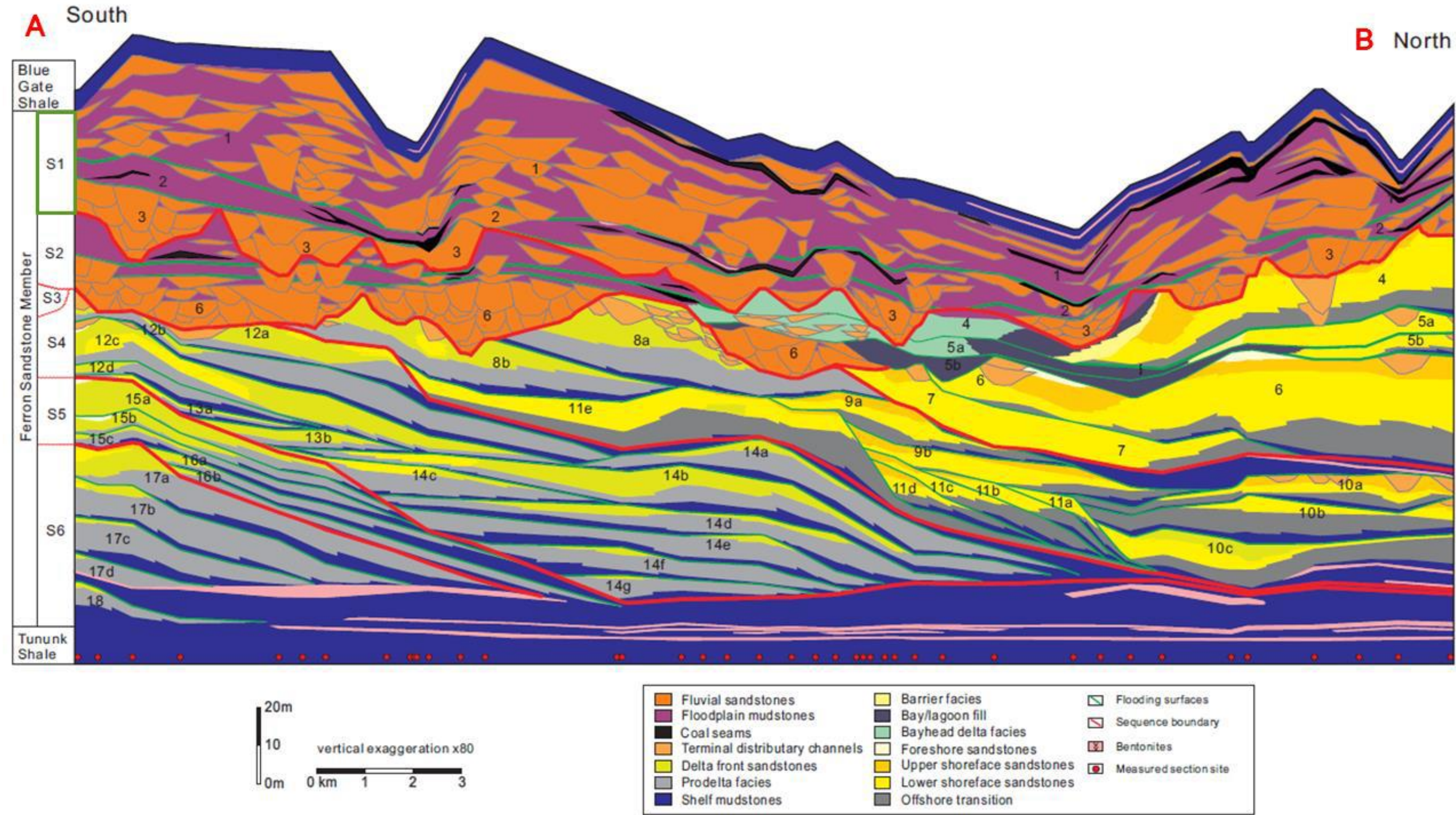


Figure. Oblique depositional dip-oriented regional stratigraphic cross section AB (South to North) through the Ferron Notom delta. The Ferron Notom delta wedge contains 6 sequences, 18 parasequence sets, 43 parasequences. Cross section by Yijie Zhu with contributions by Weiguo Li. This study focuses on S1 labeled in green bolder on left column. Figure from Zhu., 2010.

DATA

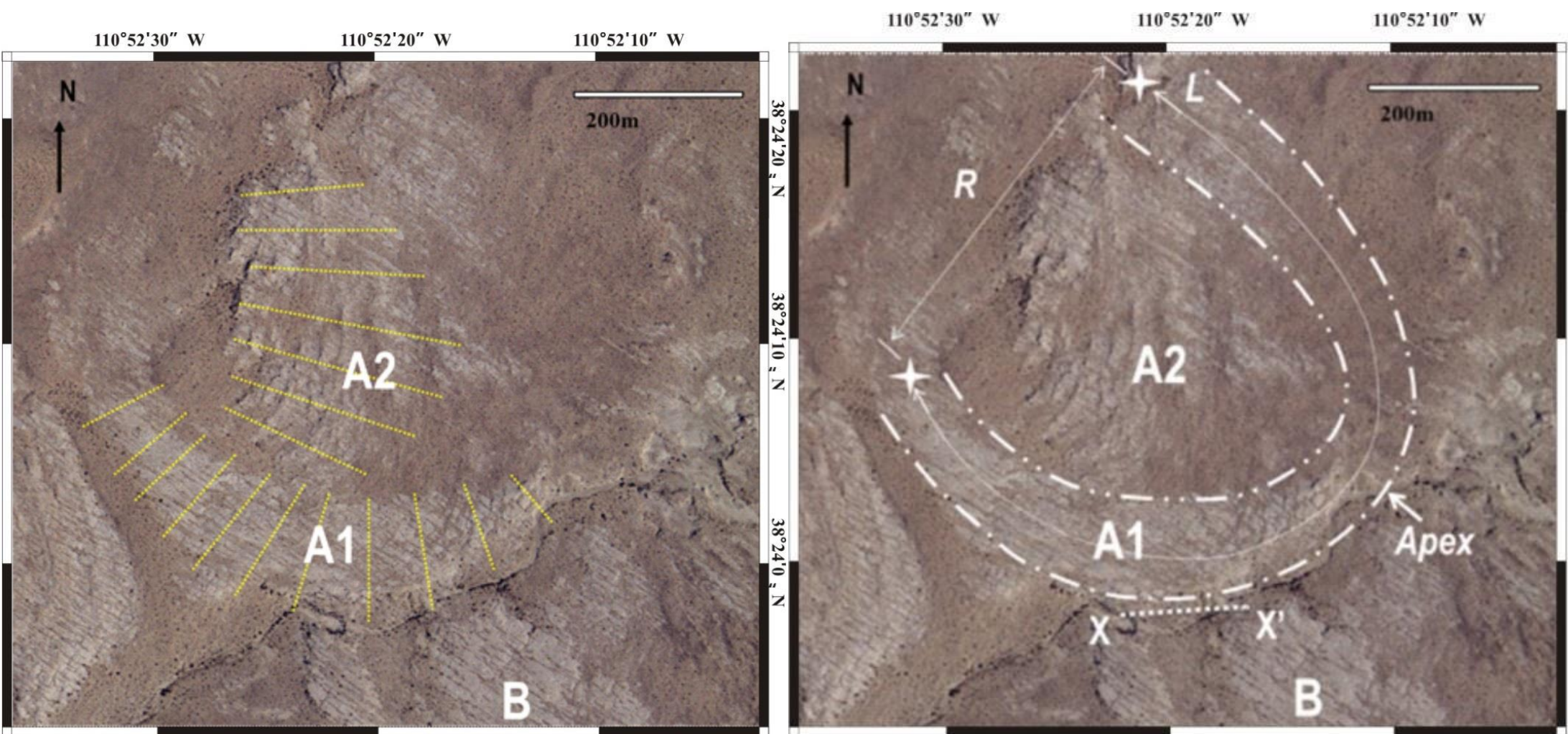


Figure. (Left) Grid system built in plan view map. (Right) Outline of three units of outcrops in field area. From the youngest to the oldest sandbody: A1, A2 and B. R (equals to λm , which is meander amplitude) represents the straight-line distance between upstream and downstream point, and L represents the actual length. Sinuosity is calculated to be 1.2 and 2.9 for A2 and A1 by dividing L by R. Bend apex and location of cross section XX' are shown.

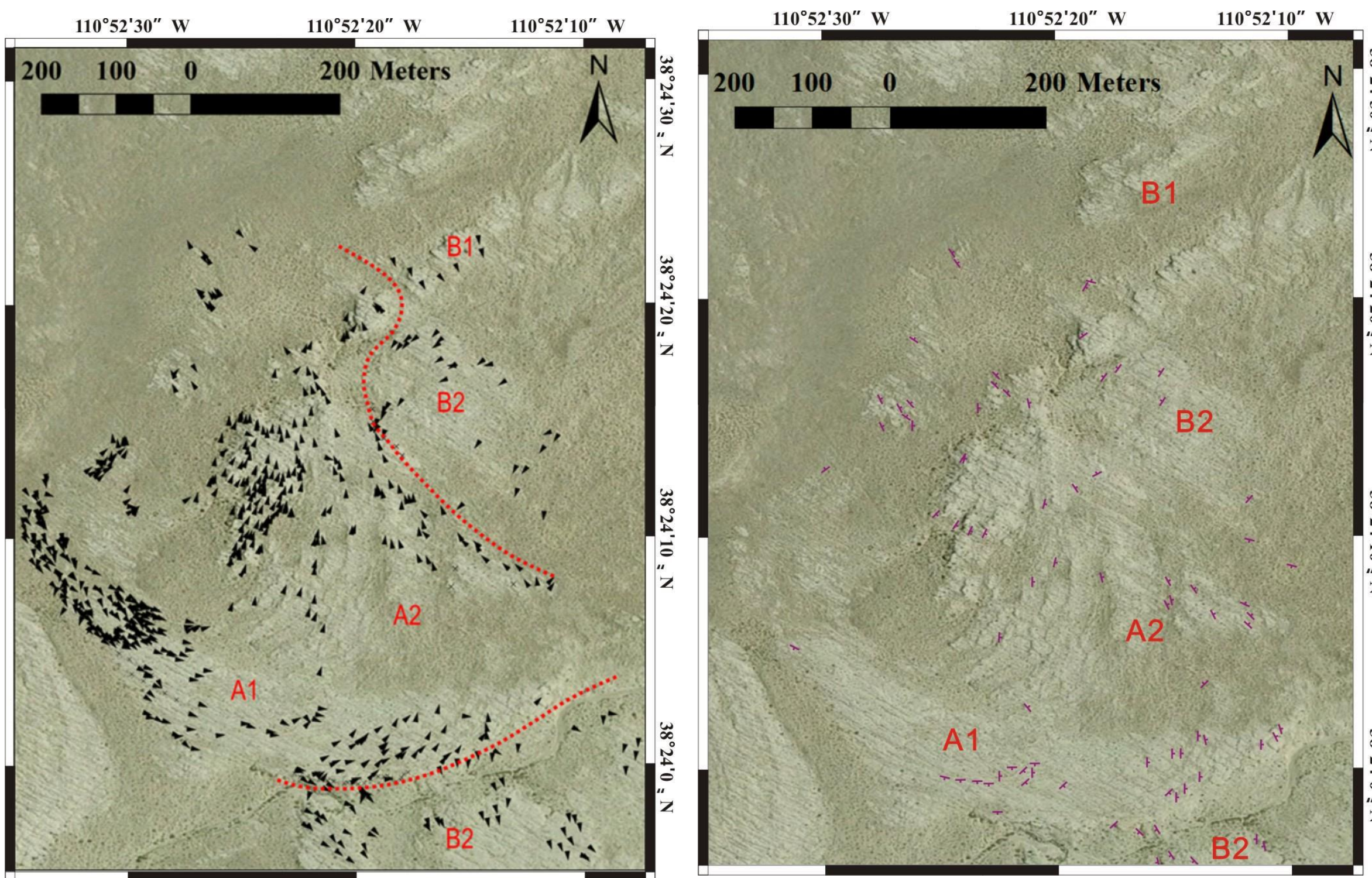


Figure. (Left) Paleocurrent variation on plan-view exposures. Red dash lines separate them in groups. Each black arrow points paleoflow direction. Paleocurrents are primarily how rib and furrow structures of exposed through cross sections. (Right) Strike and dip data of accretion surfaces.

FACIES

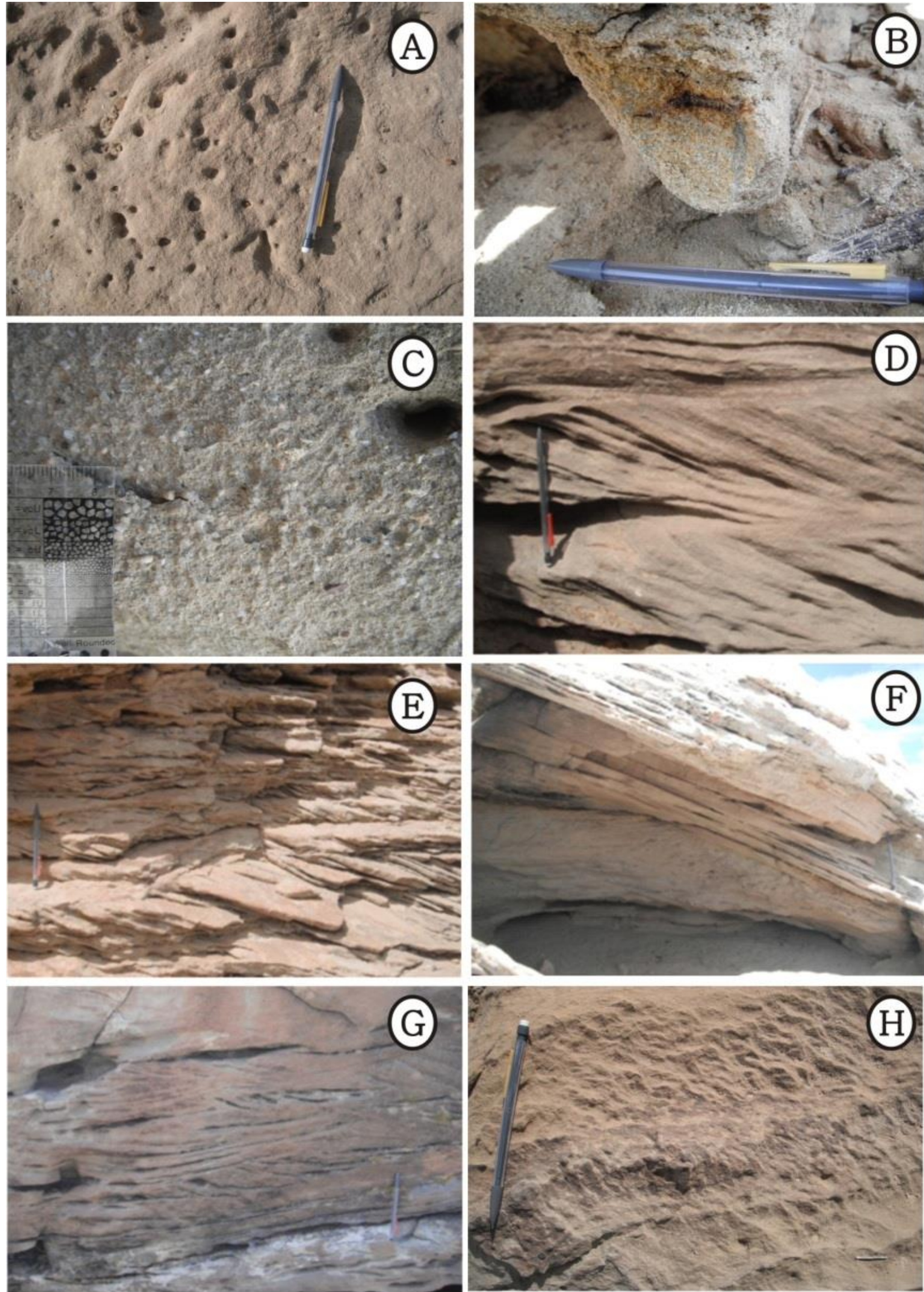


Figure. Photos showing different sedimentary structures. A) Sandstone with mud chips on top, B) Plant debris at channel basal erosion surface, C) Pebbles at channel base, D) Medium-scale tabular cross bedding, E) Centimeter thick tabular cross bedding, F) Large unit bar overlapping on horizontal laminated sandstone, G) Medium-scale trough cross bedded unit, H) Ripples in the upper part of channel bar deposit.

ARCHITECTURE ELEMENTS

- Sheet-like sandstones are mostly composed of several cross beds (mean set thickness is about 0.07m) bounded by 2nd- or 3rd- order bounding surfaces, instead of single units of cross beds bounded by 1st- order bounding surfaces. The top of these sheet-like sandbodies is characterized in plan view by a ridge and swale topography (Fig. 14A).
- Unit bars are identified by cross beds that are thicker than 1m (up to 1.5 m thick) in cliff view with foreset ribs wider than 3m in plan view (Fig. 15).
- Sand flats are mounded sandstone bodies with flat beds (Fig. 14C).

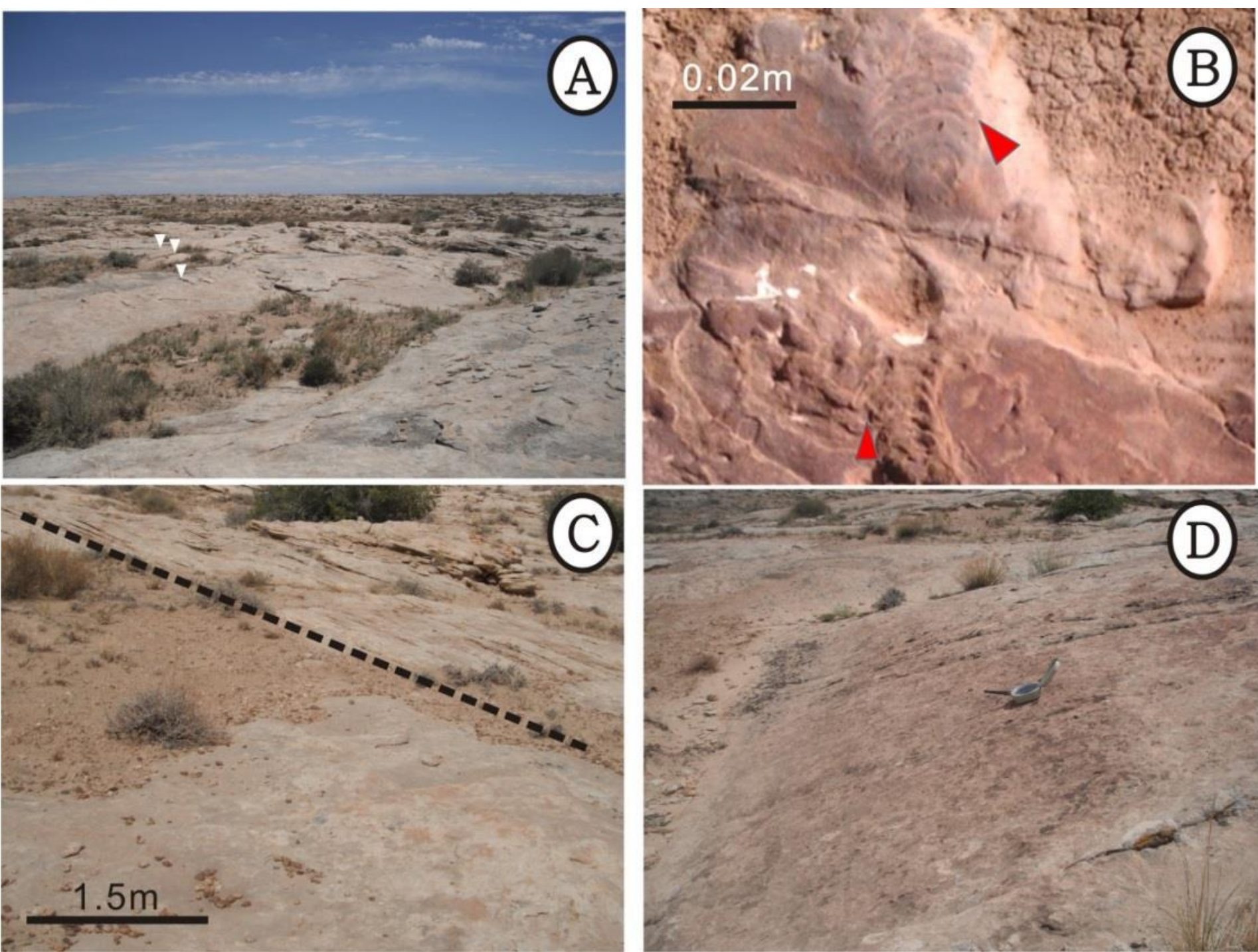


Figure. Sedimentary facies, A) Compound bar with ridge-swale topography on top, B) Beaconites preserved on a lateral accretion surface, C) Mound like sandbody in lower part of photo, D) Lateral accretion surface dipping at an angle of 25 degrees.

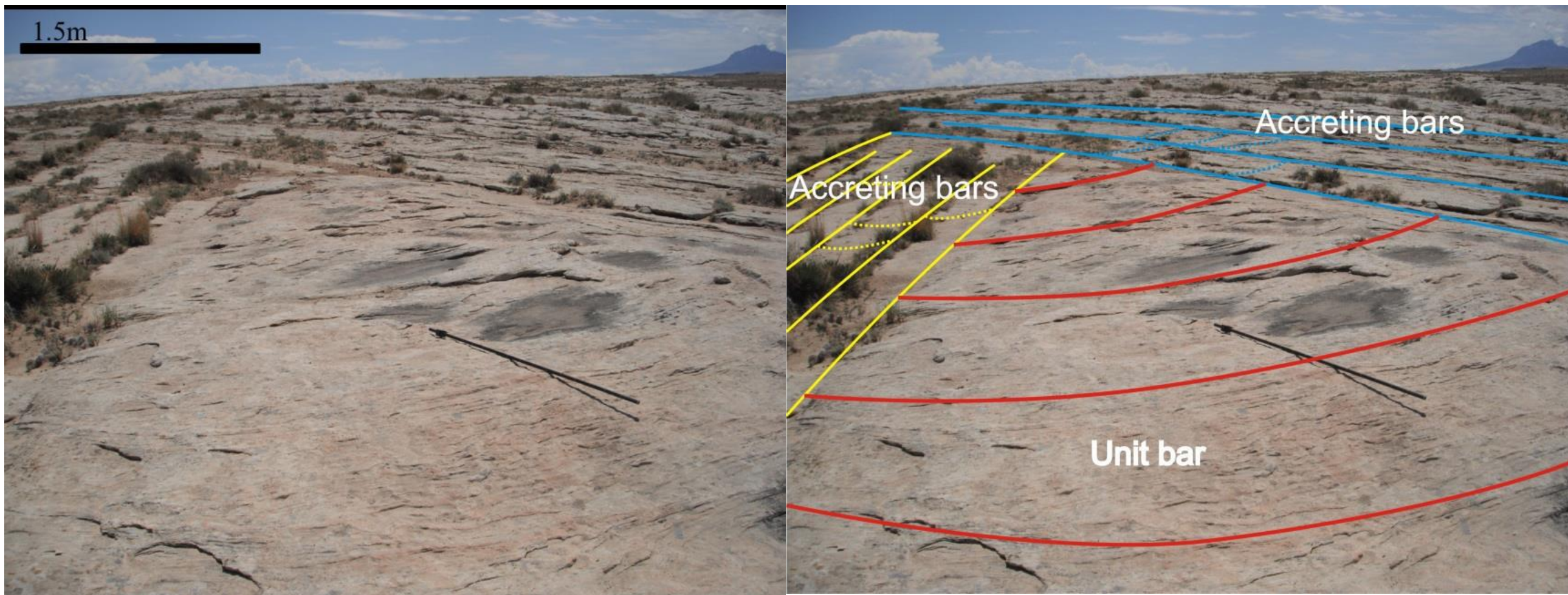


Figure. Detail interpretation of architectural element. A unit bar head is overlain by accreting bars with paleocurrent directions (obtained from dunes) perpendicular to orientation of bar accretion surfaces.



Plan-View Paleochannel Reconstruction of Ancient Meanderbelts, Cretaceous Ferron Sandstone, Henry Mountains Region, Utah

Jianqiao Wang¹, Janok Bhattacharya²

1. Colorado School of Mines, Golden, CO, United States. 2. School of Geography & Earth Sciences, McMaster University, Hamilton, ON, Canada

PALEOCURRENT VARIATION

- Channel belt B shows SSW to S then to SSE orientation. Significant relationships between cross-bedding and accreting surface are seen (Fig. 17).
- Channel belt A2 shows a NNE to N then to NNW pattern. Dips of cross-beds and accretion-surface orientations are locally nearly perpendicular to each other.
- Channel belt A1 shows a SE to E then NE pattern. Downstream accreting cross-beds are oriented at the same direction or a small angle to the regional trend.

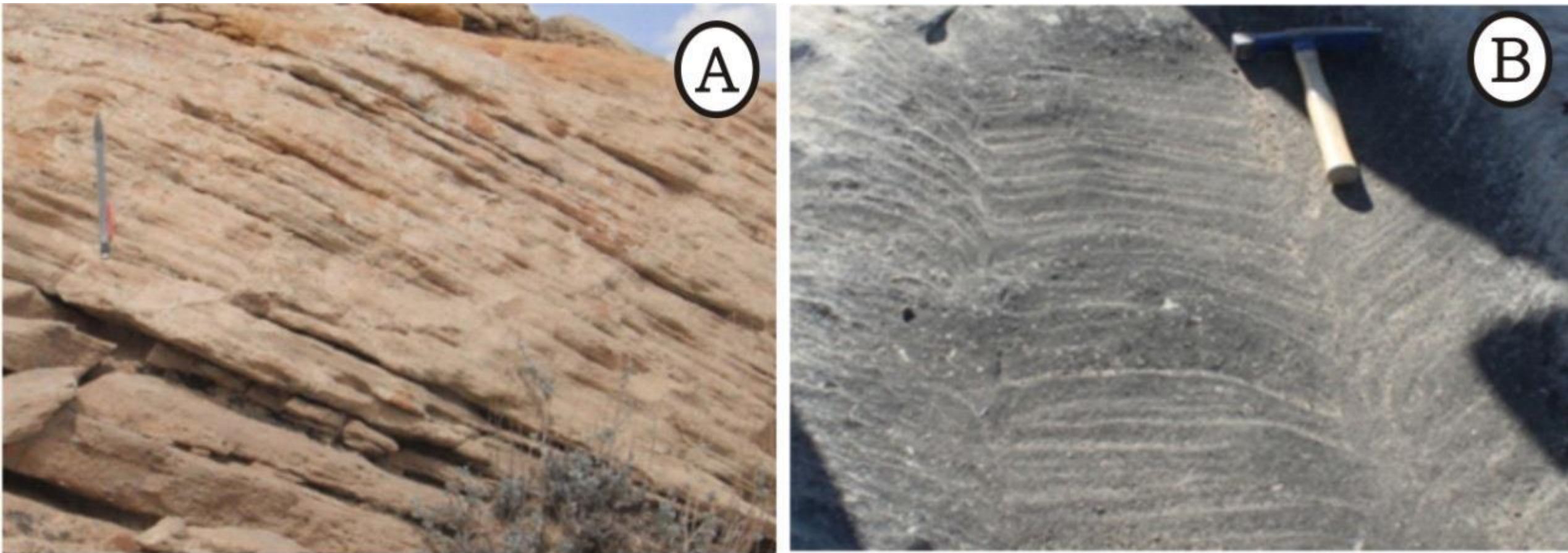


Figure. Photos showing different sedimentary structures A) Planar cross-bedded sandstone, B) Rib and furrows.

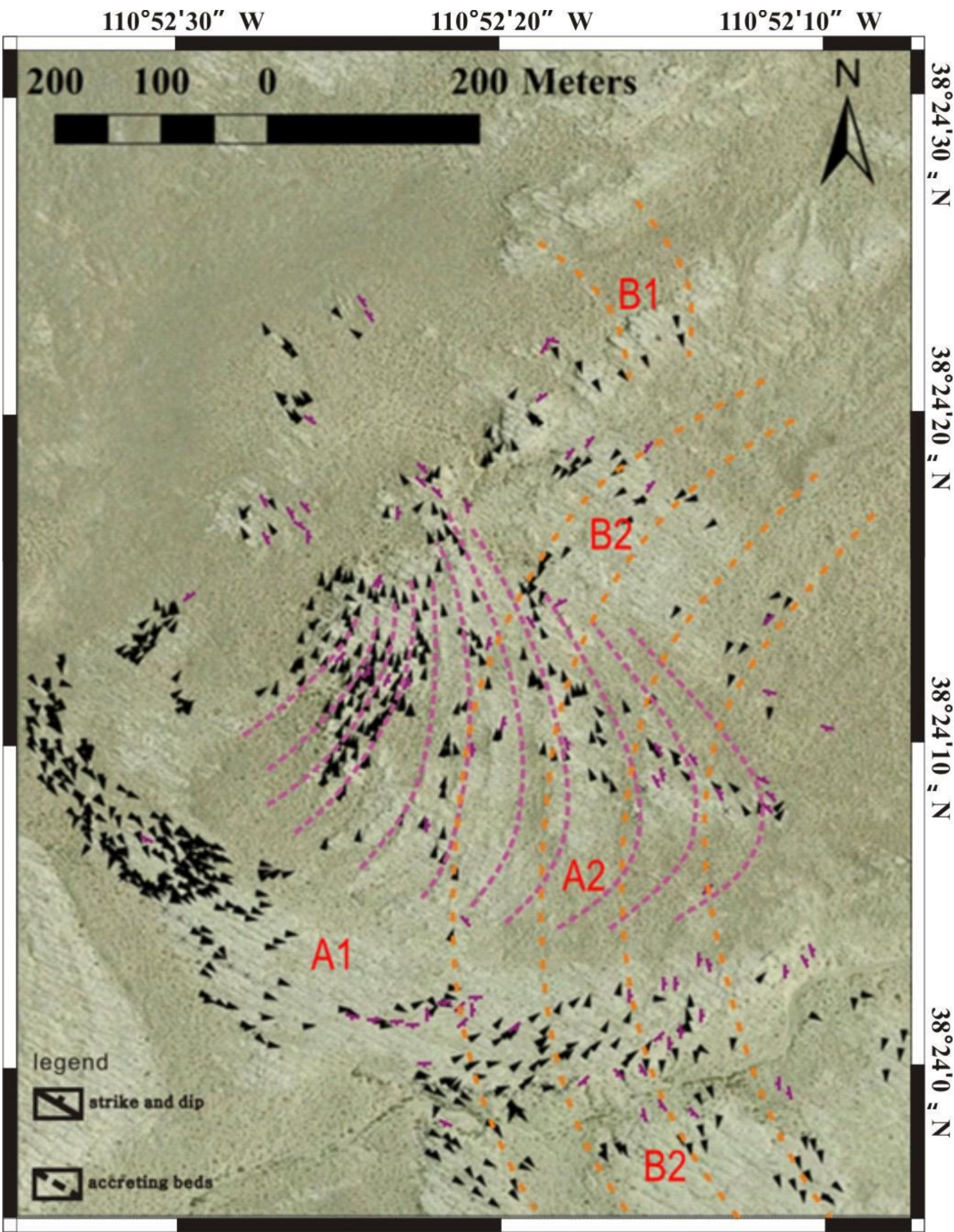


Figure. Accretion beds are shown. A combination of paleocurrent data and strike and dip data.

RECONSTRUCTING PALEOGEOGRAPHY

Generally there are three fluvial channel storeys of the Ferron river as identified. Channel A, B and C. Channel B was deposited as a reach flowing towards the south, with laterally accreting point bars preserved (Figs. 18, 19, and 20). There are two stages when Channel A and B were formed. Channel belt B1 and B2 both represent point bar deposits (Fig. 18). In the first stage of Channel A, Channel belt A2 also reveals a lateral migration pattern, but with paleoflow direction towards the north. In the second stage, compound bars and unit bars are the final deposits within the meander loop, forming Channel belt A1 (Fig. 19). The bars develop a sharp boundary towards the outside of the channel.

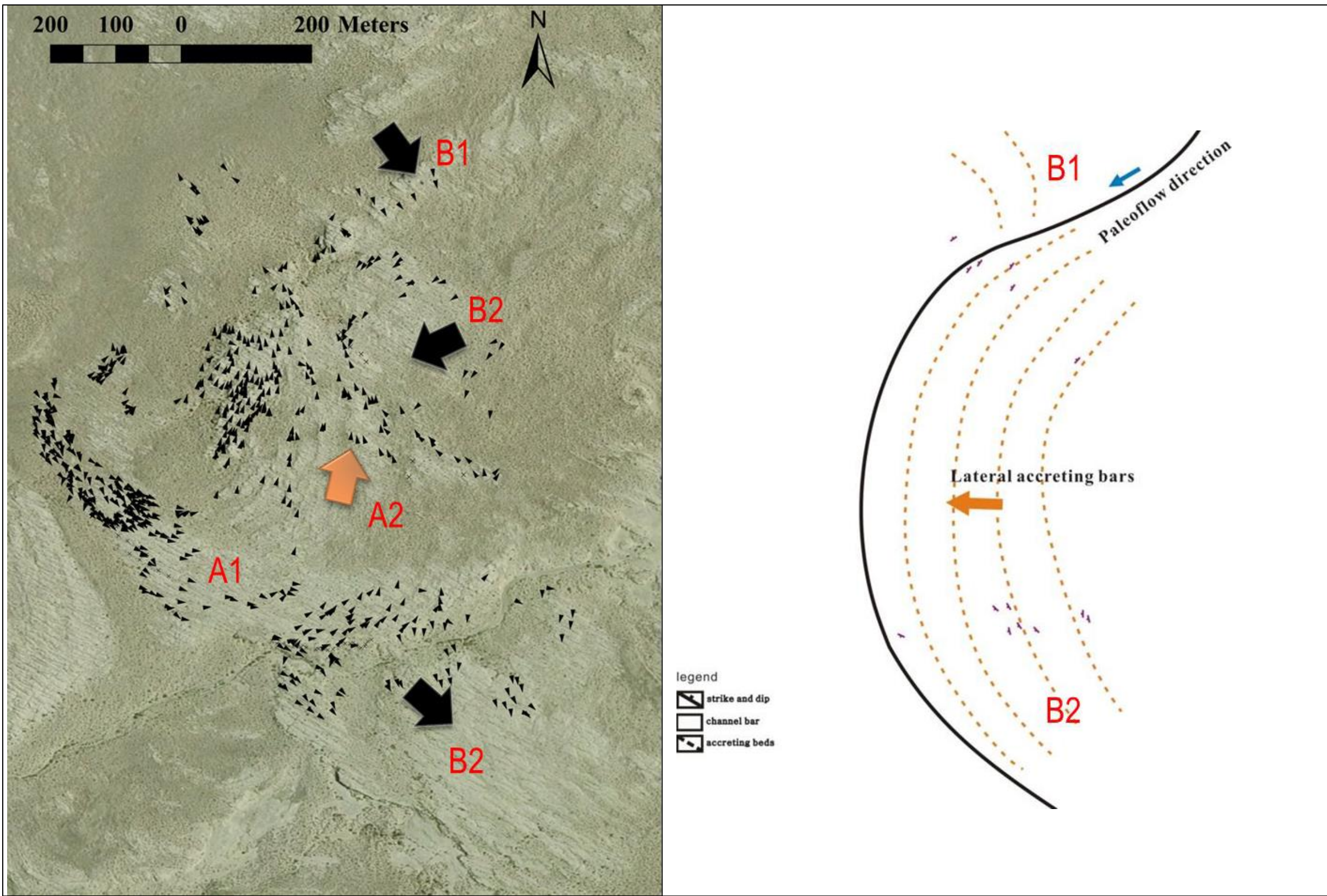


Figure. Channel belt B was flowing towards south. Big black arrows represent general paleocurrent directions observed in Channel belt B.

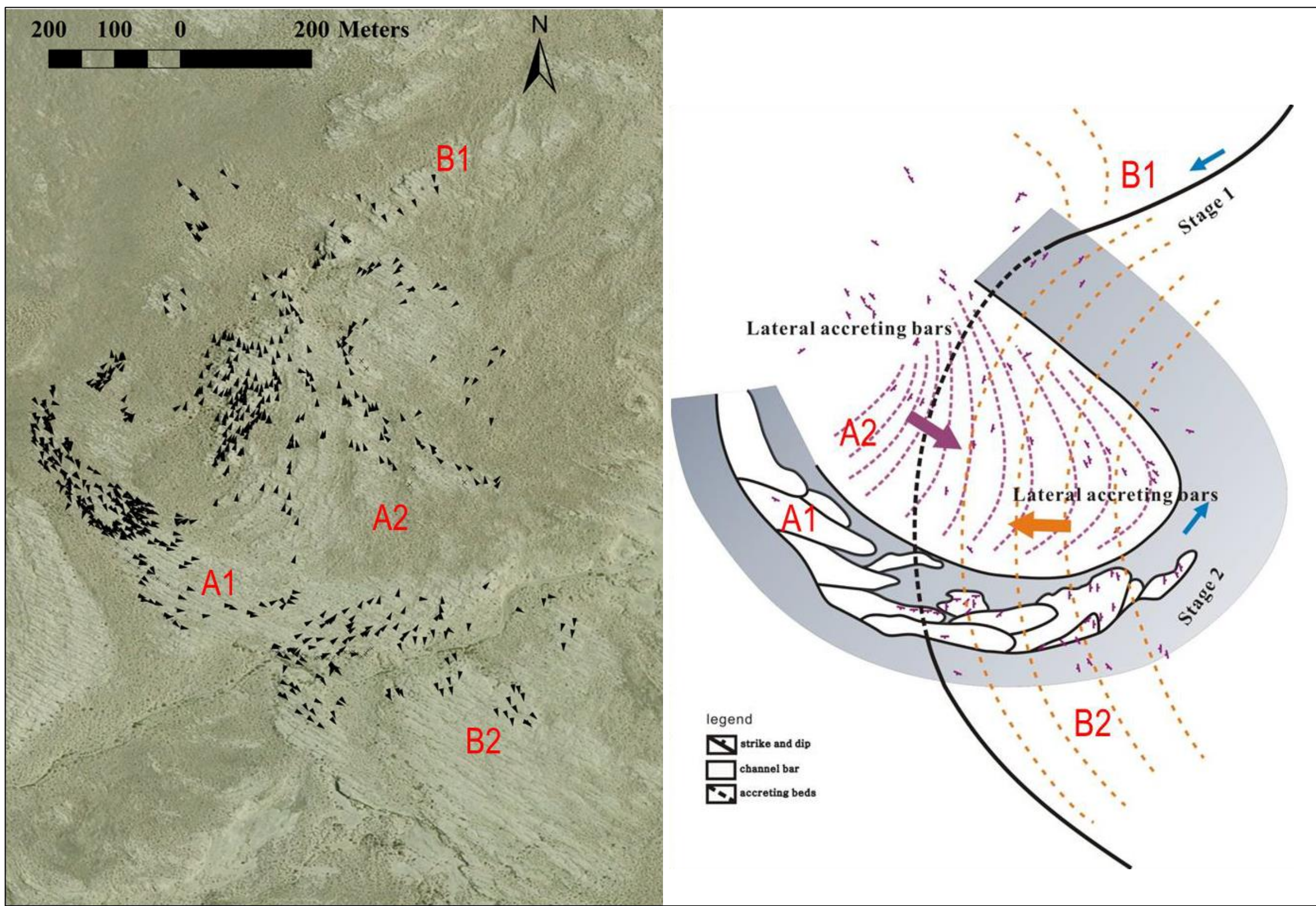


Figure. Channel A (Channel belts A1 and A2) showing different architectural elements in channel. Big orange arrow represents general paleocurrent directions of channel belt A2.

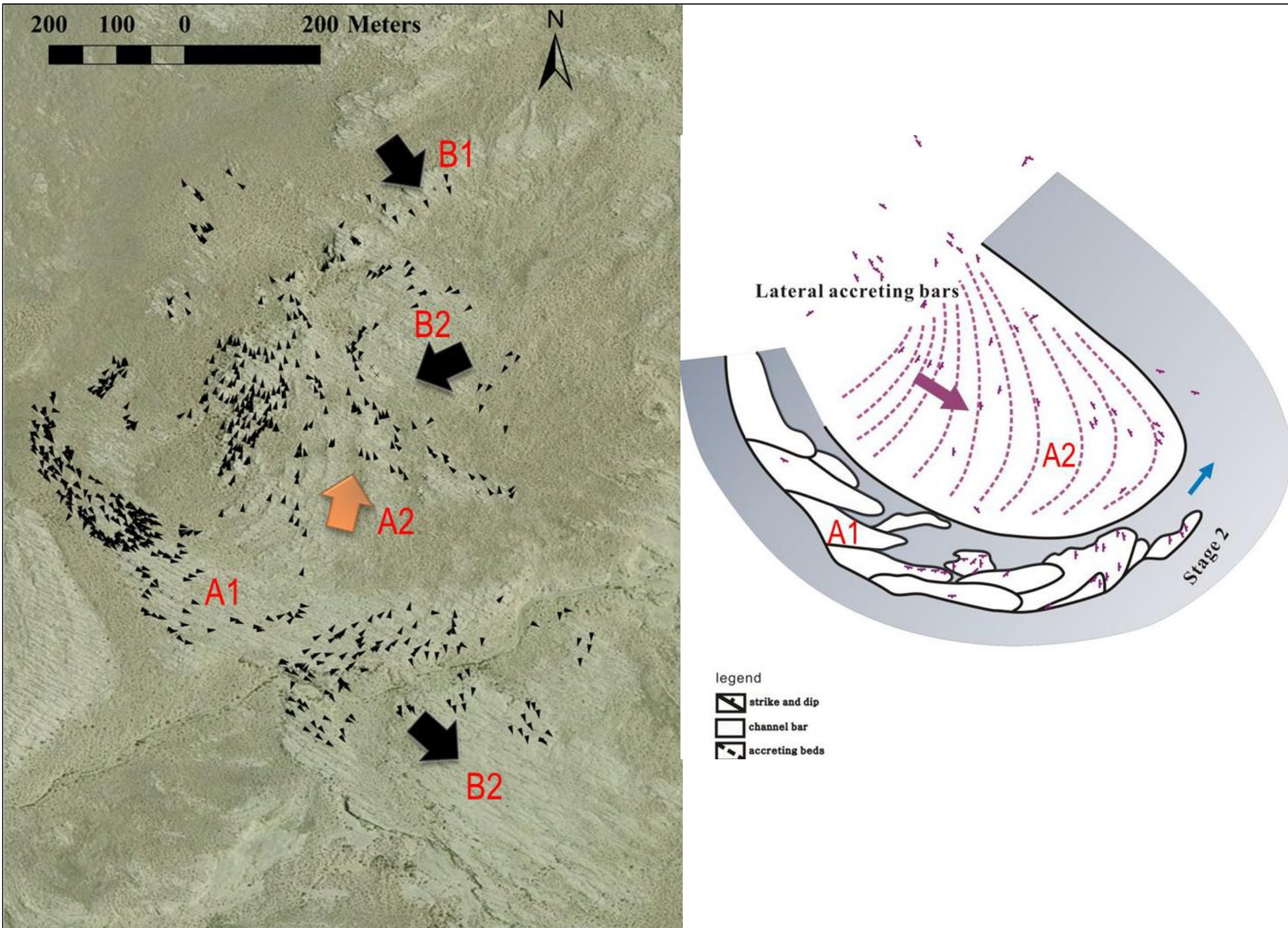


Figure. Paleocurrent variation on plan-view exposures, each small black arrow points in the paleoflow direction. Red dash lines separate different groups of paleocurrents. Lateral accretion (in orange and purple dashed lines) and plan view architectural elements are shown in detail.

ESTIMATING PALEOHYDRAULICS

Original bankful channel depth, original bankful meandering width, and meander-belt width can be either obtained from outcrop or be estimated through dimensions of a single fluvial sand body in outcrop by applying these equations 1, 2, and 3:

- Equation 1. $H_m = 5.3B + 0.001 B^2$, where H_m =mean bedform height, B = $S_m/1.8$, S_m =mean cross-set thickness. An application of this relation proposed by Leclair and Bridge (2001) to estimate flow depth independently from cross-set thickness is tested in this study.
- Equation 2. $D = D^* \times 0.585/0.9$, (Ethridge and Schumm, 1977), where D =Original bankful channel depth, D^* =Average thickness of the main point bar.
- Equation 3. $W = W^* \times 1.5$, (Allen, 1965), where W =Original bankful meandering width, W^* =Average horizontal width of the lateral-accretion surfaces as exposed in outcrop.

Measurement of cross-set thickness obtained from cliff exposures makes it now possible to derive a relatively robust estimate of channel depth from the application of equation 1. Using the average cross-set thickness of 0.13m and 0.08m for Channel belt B and A2 respectively suggests that the range of channel depth is 2.3m to 3.9m and 1.5m to 2.5m, assuming flow depth of 6 to 10 times mean dune height, which is calculated to be 0.38m and 0.25m for each. Average flow depth is 3.1m and 2.0m for each.

An alternate way to estimate original bankful channel depth of Channel belt B is using average thickness of the main compound bars obtained directly from the three measured cliff sections, which is 3.4m, and the depth turns out to be 2.2m. Estimated point bar thickness can be used to calculate original bankful channel depth by applying the equation

- Equation 4. $D = D^* \times 0.585/0.9$, (Ethridge and Schumm, 1977). Channel belt A1 is dominated by downstream accreting braid bars, and the technique is thus only applicable for Channel belt A2. Channel belt B was not considered for bankful channel width estimation using Allen's equation (1965), because there are not enough well exposed accretion surfaces in Channel belt B. Allen's equation (1965) can be applied to point bars in channel belt A2, whereas downstream accreting compound bars are dominant in Channel belt A1, therefore data was only collected in Channel belt A2 for the empirical equation test.

By using average flow depth of channel A (3.1m) and minimum dipping angle (3°), the average horizontal width of lateral accretion surfaces in exposed point bars in Channel belt A2 is approximately calculated to be 60m, which yields a bankfull channel width of 90m using $W = W^* \times 1.5$, (Allen, 1965). This allows the following comparison between field measurements vs. empirical equations.

Meander amplitude (λ_m) can be obtained independently from measurements on plan view maps, which is about 1083m for Channel B, and 435m for Channel A, whereas the calculated result is 981m for Channel belt A if using Equation 5.

- Equation 5. $\lambda_m = 10.9W^{1.01}$ (units=m), (Leopold and Wolman, 1960), where λ_m =Meander amplitude (meander-belt width), W =Bankfull channel width.

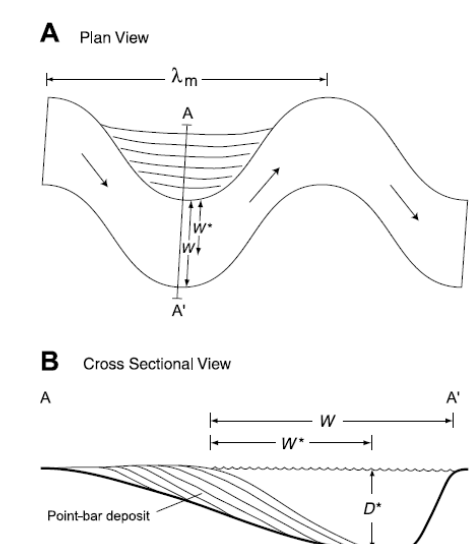


Figure to the left. Schematic illustration of a meander bend in (A) plan view and (B) cross sectional view. Geomorphic parameters include bankfull channel width (W) and meander wavelength (λ_m). Bankfull channel depth and width are estimated from point-bar deposits in outcrop using the point-bar thickness (D^*) and horizontal length of lateral-accretion surfaces (W^*). Based on Lorenz et al. (1985).

Table. Calculated paleohydraulics parameters from outcrop data

Application of Leclair and Bridge, 2001	Average cross-set thickness	Average dune height	Average flow depth	Flow depth range	Average bar thickness	Original bankful channel depth
Channel A	0.05m	0.25m	2.0m	1.5-2.5m		
Channel B	0.08m	0.38m	3.1m	2.3-3.9m	3.4m	2.2m

Table. Discharge estimation and meander amplitude measurement

Field measurement	Width of lateral accreting surface	Bankful channel width	Average discharge area	Average discharge	Meander amplitude
Channel belt A1	60m	90m	180m ²	180m ³ /sec	435m
Channel belt B					981m

River discharge is given by the equation $Q = A \times U$, where Q =Discharge, A =Cross sectional area of the channel (Width \times Depth), U =Average velocity. Moreover, Q can also be estimated using the equation of Matthai, (1990): $\log Q(\text{flood}) = -0.070(\log A2) + 0.865 \log A + 2.084$, where A is the area of the drainage basin. An alternative method for estimating Q_w in an ancient system is presented by Bhattacharya and Tye, (2004), Bhattacharya and MacEachern, (2009), and Davison and Hartley, (2010). Dischington (2013) used the Law of the Wall to estimate average flow discharge by calculating average flow velocity of water through multiple rectangles across a channel. Equation $Q = A \times U$ is used in this study for estimating average river discharge.

Channel belt A2 provides estimates of channel depth and channel width to make an estimation of annual discharge of the Ferron river. An approach to estimate flow velocity by using bedforms, grain size, and water depth use the 3D bedform diagram of Rubin and McCulloch (1980). Dunes are the dominant stable bedform in Channel belts A1 and A2, and reconstructed original flow depth of channel A is 2m. Grain size is fine to medium sandstone. Using these parameters, 100cm/sec (1.0m/sec) is used as an estimate of average flow velocity. Applying U as 1.0m/sec and A as 135~225m² (Bankful channel width 90m multiply flow depth 1.5~2.5m) to equation $Q = A \times U$, an average discharge Q_w of 135~225m³/sec is calculated.

With respect to the order of magnitude of average discharge, the calculated value (less than 300m³/sec) is considerably smaller than the discharge of 1000m³/sec, which has been proposed by Ashworth (2012) and Latrubesse (2008) to define big rivers. The Ferron river has been demonstrated to have water depth less than 9m by Bhattacharya and Tye (2004) and Bhattacharya and MacEachern (2009). An average discharge of the largest Ferron river in the Last Chance system, which is 10m deep and 150m wide, is documented as 1500 m³/sec. Li (2010) evaluated paleodischarge of V1 and V2 in Ferron system, which is 420~1290 m³/s and 110~310 m³/s respectively. The smaller dimensional Ferron river in the study area is comparable to Li's result. It may have little chance to belong to the trunk river system, staying within valley, for it has unconfined channel deposits with a high sinuosity.

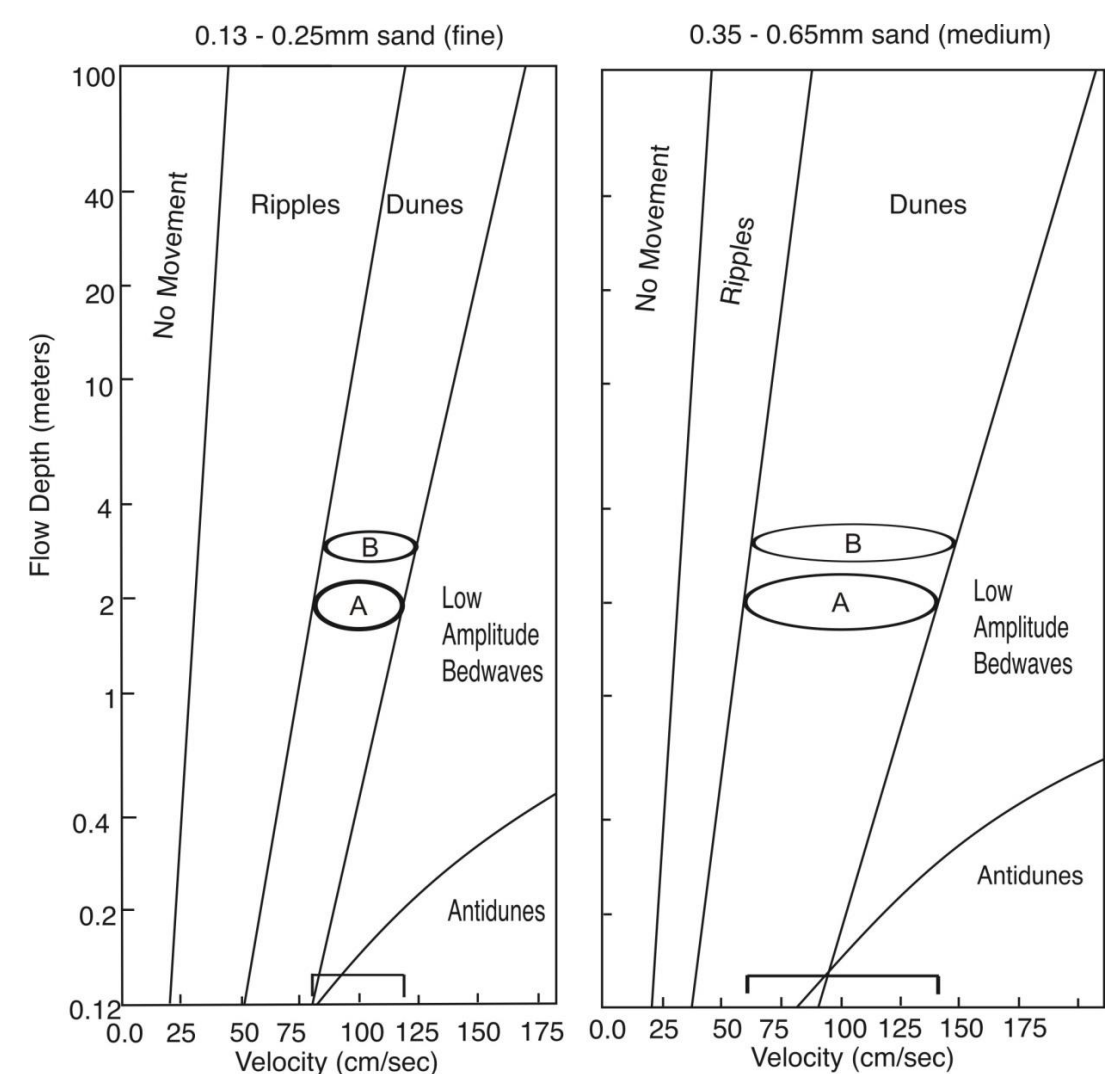


Figure. Grain size variation corresponds with flow depth and velocity.



Plan-View Paleochannel Reconstruction of Ancient Meanderbelts, Cretaceous Ferron Sandstone, Henry Mountains Region, Utah

Jianqiao Wang¹, Janok Bhattacharya²

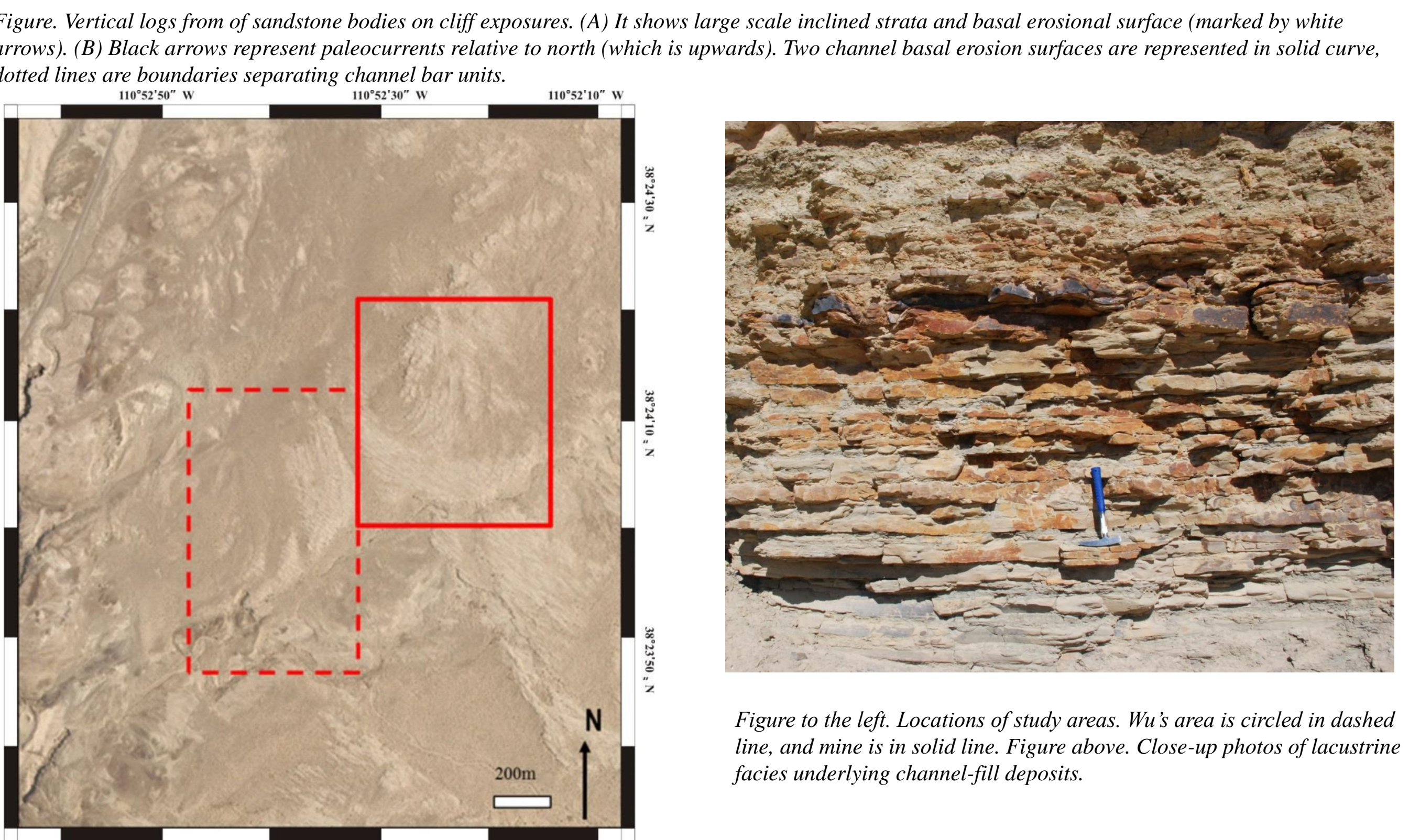
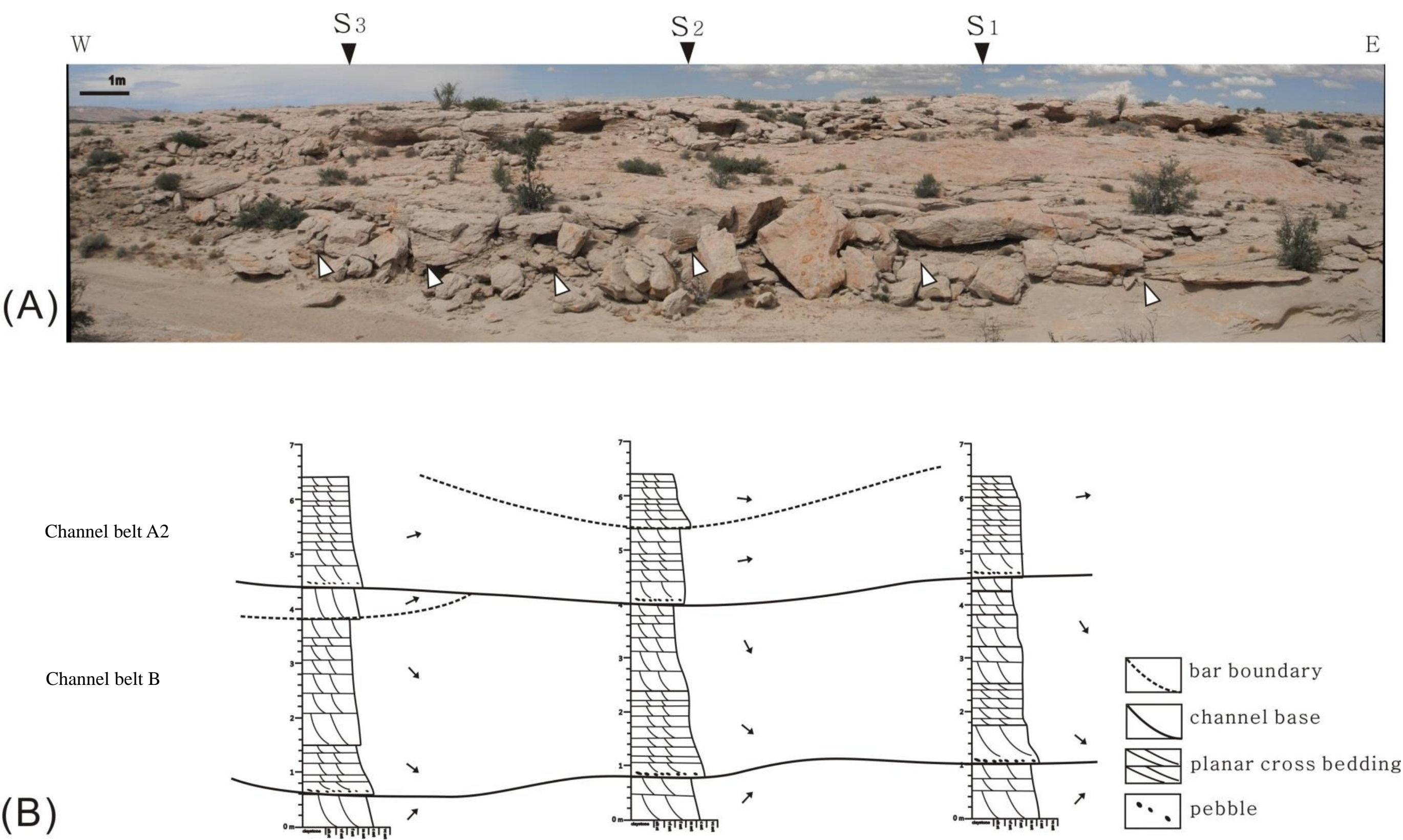
1. Colorado School of Mines, Golden, CO, United States. 2. School of Geography & Earth Sciences, McMaster University, Hamilton, ON, Canada

VERTICAL SUCCESSION

Three fining upward fluvial successions were observed in vertical sections. They may not be fully preserved in all sections due to erosion, Sandstones are wedge shaped as appears on the middle part of the measured section S3. Some pass laterally at their upper edges into thinner wedges of sandstone.

The middle and upper fining upward facies successions are composed of lower medium to lower coarse sandstone. Medium to large scale planar cross strata, with set thickness ranging from 0.2m to 1.5m, but commonly 0.1 to 0.5m are observed as the dominant internal structure of the large-scale cross sets (lower parts). The upper strata within a fining-upward succession are very fine to upper fine sandstone, and generally contain tabular cross strata (set thickness ranges from 0.02m to 0.2m) in dip view or small scale trough cross strata in strike view (set thickness is about 0.15m). Mud chips, plant debris, and intraformational pebbles are also commonly found at basal erosive surfaces.

In the lower fining upward facies successions, dune-scale trough cross beds are commonly seen. Medium-scale tabular cross strata (mean thickness is about 0.3m) is observed on the cross section.



MODERN ANALOG

The sandy braided South Saskatchewan River is characterized by a variety of barforms (Ashworth et al., 2011). Like elementary units found in the Ferron river, singular unit bars and complex compound bars are identified via areal images, and field data were collected to describe the sedimentology and evolution of both. Discharge data from the South Saskatchewan River matches the order of magnitude with that calculated for the Ferron rivers.

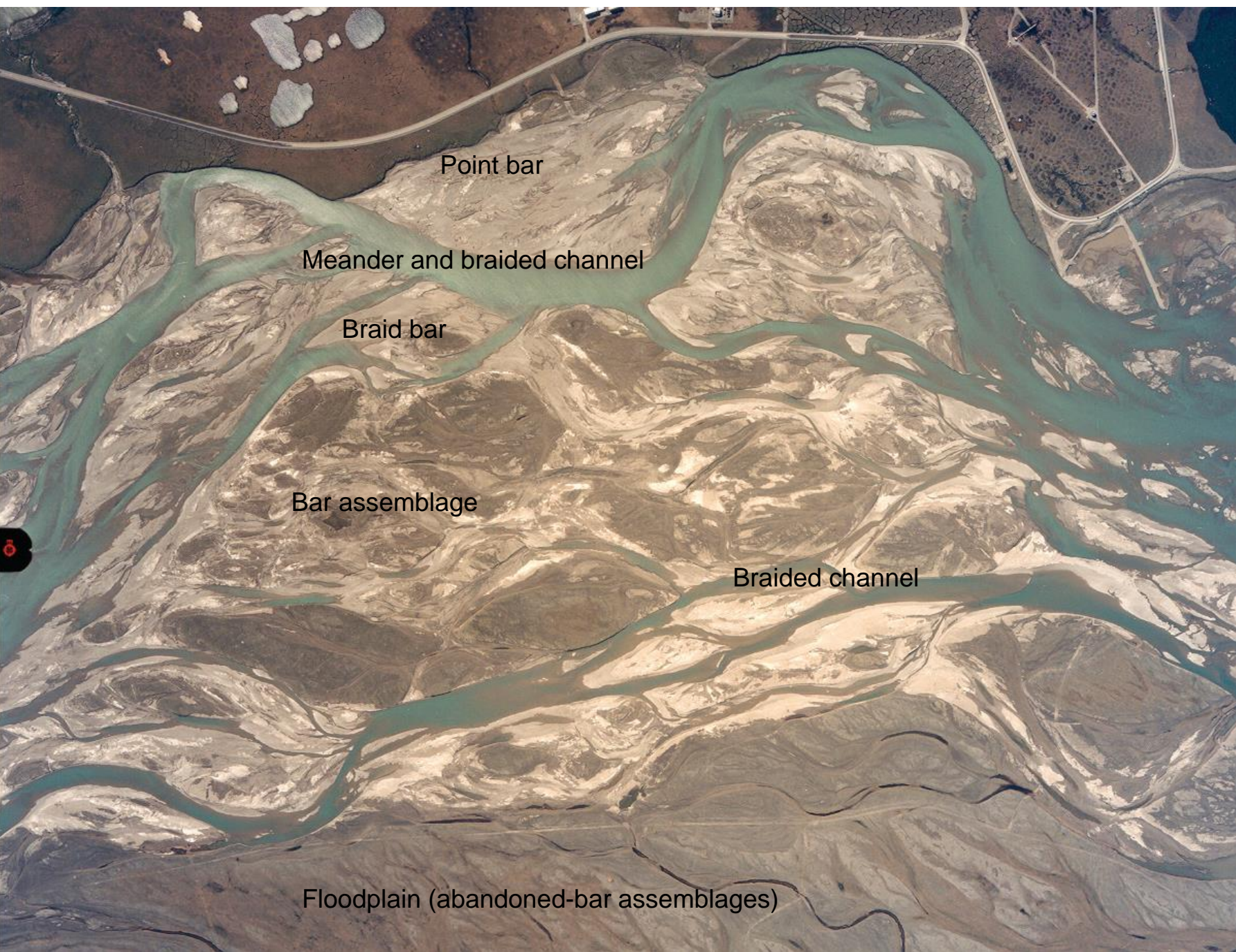


Figure. Sagavanirktok (northern Alaska, U.S.A.) channel belt (2 km wide) Compound bars have accretion topography indicating downstream translation and lateral growth, and channel fills are also evident.

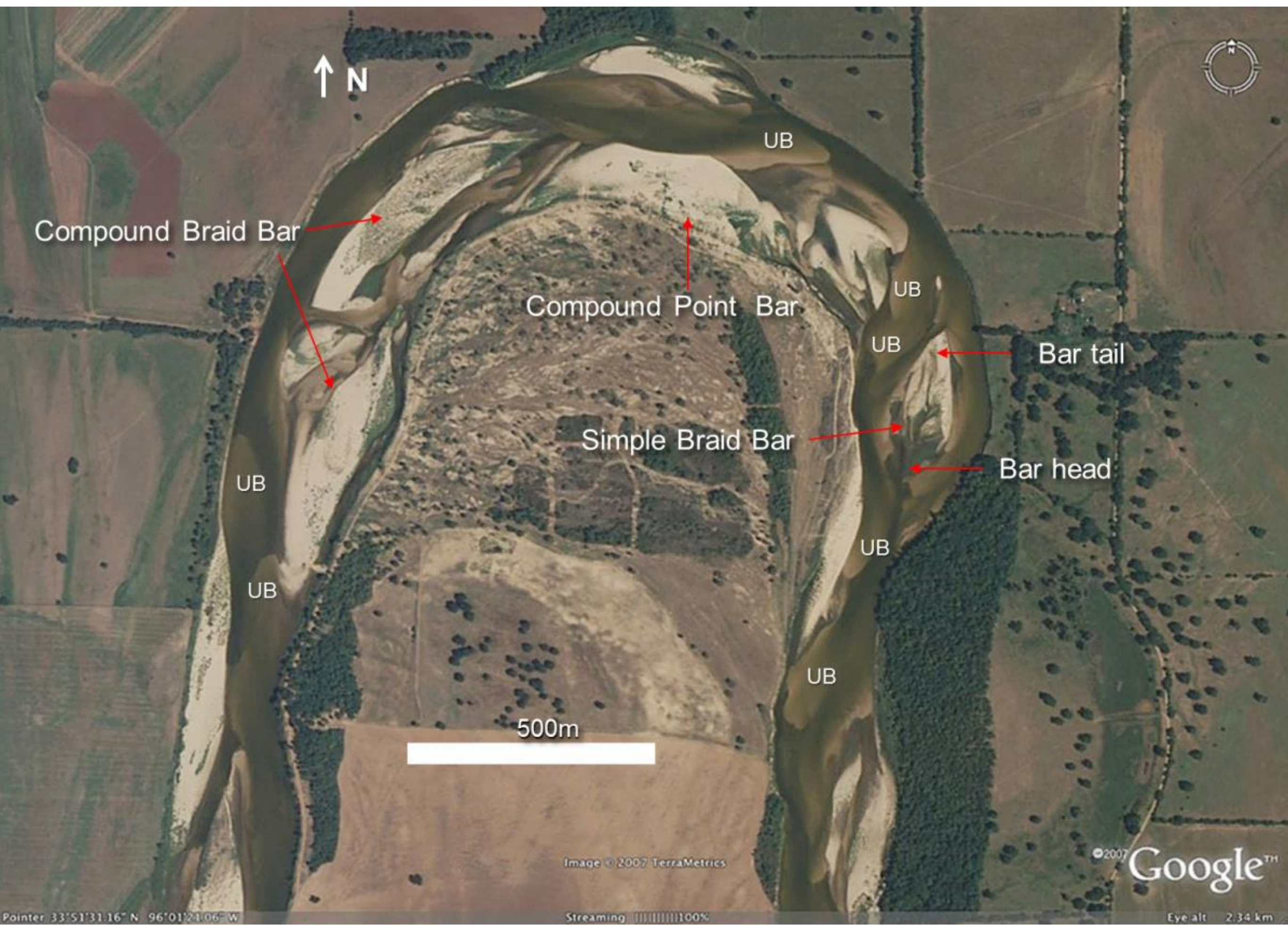


Figure. Google Earth picture of Red River. UB = unit bar.

GRAIN-SIZE VARIATIONS IN PLAN VIEW

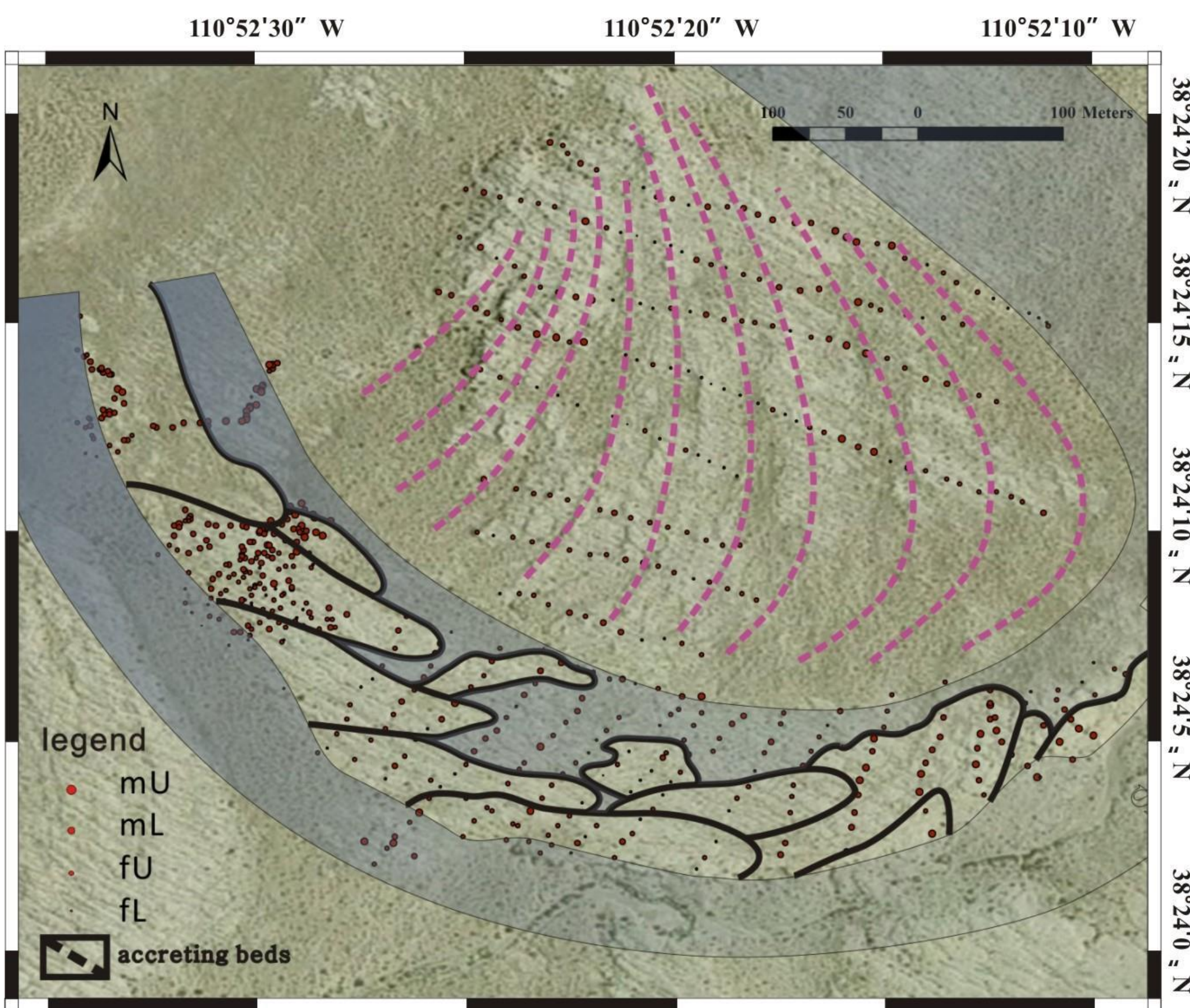


Figure. Grain size variation integrated with plan view interpretation of channel belts and bars. Small bars in A2 and unit bars in A1 are numbered. Area covered by water is shown in grey, representing channel fill with lower energy.

Along the river reach in A2, there is an apparently general coarsening trend towards the apex within some meander loops (from meander scroll No. 6 towards No. 9 in Fig. 24), which consists only of point bar deposits. Also, as the channel migrates towards the bend apex, the sinuosity increases gradually from moderate to high. However, it is hard to demonstrate any significant difference of grain size variation in each loop. Grain-size distribution shows a relatively scattered pattern in Channel belt A1 (Fig. 24). Sediments of the largest grain size are located at the east side of A1 (close to the bend apex, in bars No. 11, 12, and 13, Fig. 24).

The dual components of compound bars and unit bars in Channel belt A1 makes it difficult to find simple fining upward and downstream trends. Grain size in Channel belt A2 shows a high degree of variation associated with the ridge and swale topography (Fig. 24). Both channel belts have downstream fining trends, at least in the bar scale. In A2, grain size decreases downstream within meander scrolls No. 5 and No. 6, but the trends are less clear in the other scrolls.

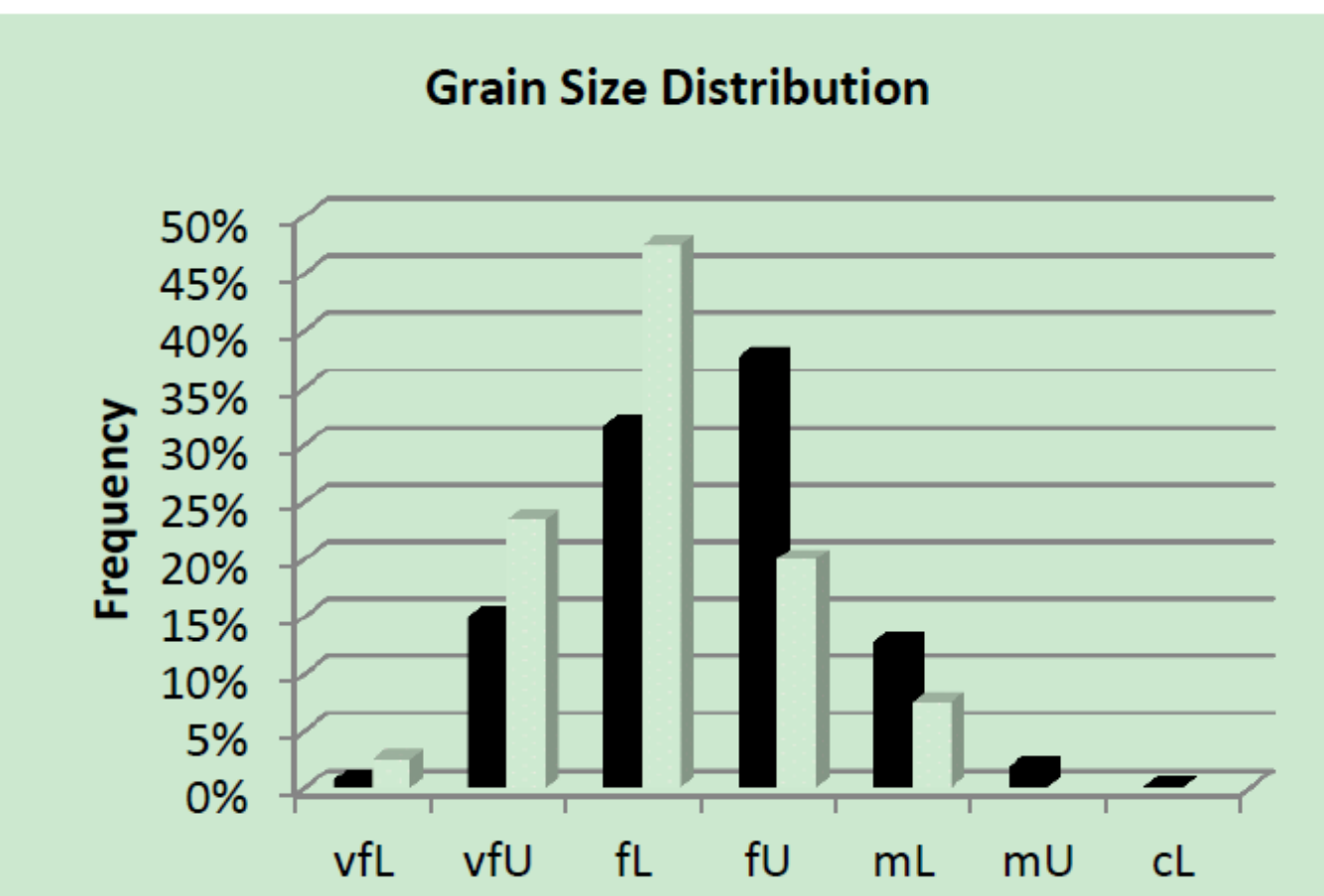


Figure. Histograms of grain size data (1259 samples totally) collected from top surfaces of channel belt A1 (in dark black) and channel belt A2 (in white).

CONCLUSION

The Ferron rivers are small to medium scale, according to the obtained paleohydraulic parameters ($Qw = 135\sim 225m^3/sec$). There are three stories of channel deposits (Channels A, B, and C) identified in the study area. The youngest one (Channel A) is 2.0 m in depth, 90m in width, 435m in meander amplitude, and has a sinuosity of 2.9. The middle one (Channel B) is 3.1m in depth, 1083m in meander amplitude, and has a sinuosity of 1.2.

“Text-book” style channel and bar geometries constitute most of the Ferron river sandstones (Channel belts A2 and B) in our study area. The lateral amalgamation of many point bars suggests the dominance of a meandering river style, in which sinuosity is moderate to high in Channel belt A2, whereas it is low in Channel belt B. Compound braid bars built by overlapping unit bars constitute the final youngest channel deposits (Channel belt A1), which do not have “text-book” point bars.

Topographic roughness is more significant in the higher sinuosity bend (A2) than the lower sinuosity one (B). There is limited grain size variation across-channels observed in the Ferron channel belts, compared to fining upward successions observed at the unit bar scale. Besides, grain size coarsens towards the bend apex in Channel belt A2.

The calculated meander wavelength (981m) is close to the independent measurement (1083m) based on plan view exposures. The increasing horizontal width of laterally accreting surfaces towards the bend apex results in little divergence of channel width estimation. The measurement from the plan-view map only suggests the value for the last stage of flow, while 981m is calculated from mean values of widths.

ACKNOWLEDGEMENT

This study represents part of the results of consortium funded research to the University of Houston Quantitative Sedimentology laboratories (QSL), which includes Anadarko, BP, BHP, Shell, Nexen, Pioneer, Inpex and ExxonMobil as current supporters. I would like to thank my supervisor Janok Bhattacharya, and my colleague Ben Browning, Ben Hilton, Cameron Griffin, Chenliang Wu, Danfix D’Souza, Daniel Garza, Shahidullah Abu, Yangyang Li who have shared their knowledge as applied to the Ferron in the field.

